Copyright © 2017 by American Scientific Publishers

Journal of
Nanoelectronics and Optoelectronics
Vol. 12, pp. 1–8, 2017
www.aspbs.com/jno

ARTICLE

Temperature Sensors Based on One Dimensional Photonic Crystals with Different Double Defects

S. E.-S. Abd El-Ghany

In this paper the transmission properties in the Uv, visible and infrared (IR) spectra for one-dimensional photonic crystals with different double defects, under the effect of temperature variations has been theoretically studied. Numerical calculations were carried out by using the transfer matrix method (TMM). The multilayer system, air $(Si/SiO_2)^N$ D_1 $(Si/SiO_2)^M$ D_2 $(Si/SiO_2)^L$ Glass, has been taken as temperature dependent. The numerical results showed that the number of PBG was increased by increasing the degree of temperature variation. In addition, the variation of temperature caused shifting of the photonic pandgaps to higher wavelengths which can be exploited in the design of temperature sensors.

Keywords: Photonic Crystals, Photonic Band Gap, Transfer Matrix Method.

1. INTRODUCTION

Investigations on the properties of photonic crystals, particularly photonic band gap of different materials, have become an area of interest for many researchers.[1–3] Photonic crystals are periodic layered structures which can be classified as one, two or three dimensional PCs. The photonic band gap (PBG) in a Photonic crystal is like to the electronic band gap in a solid as there is analogy between the structural periodicity of a PC and the periodic arrangement of the atomic potential.[4] The existence of wide band gaps in Photonic crystals has different applications such as optical switches, optical filters, wave guides and reflector.[5–9] This behavior has opened up important possibilities for the design of novel optical and optoelectronics. The PBG can be tuned by means of some external agents. It can be changed by the operating temperature (T-tuning). A superconductor/dielectric PC belongs to this class of Photonic crystal. Liquid crystals and semiconductors can be used as a one of the constituents of a PC. Semiconductor doped by impurities is more important than the pure ones for various applications in PCs. These doped photonic crystals present some resonant transmittance peaks in the band gap corresponding to the occurrence of the localized states. This is because of the change in the interference behavior of the incident waves. Defects can be introduced into PCs by changing the thickness of the layer, inserting another dielectric layer or removing a layer.[10]

Due to the simplicity in 1D PC fabrications over 2D and 3D PCs, the defect mode can be easily introduced within 1D Photonic crystals. Such design can be used for various applications, such as TE/TM filters, splitters, in fabrication lasers and in light emitted diode.[11–14]

From the applications of the (PC) sensors in the industrial systems, a photonic nanocrystal can connect with the industrial equipment and monitor the parameters critical to the efficiency of the equipment. These efficiencies based on a combination of measurements such as temperature, pressure, refractive index, expansion and so on. These data are transmitted to a sink node which analyzes the data from each sensor.[15]

Hydrothermal route is a promising method for the direct preparation of nanostructures. This is because the generation products highly crystalline purity, narrow size and high surface area.[16] This is one from the methods which can be used in the preparation of photonic nanocrystals.

Kennedy et al.[17] used the hydrothermal method for growing ZnO crystals obtained from Semi-Wafer, Inc. were implanted with 40 keV Gd ions. The doping concentration can be changed in the near surface of layers. This leads to that; the moment per unit area can be changed as a function of temperature. This technique gives another form of sensors.

Alatas et al.[18] have been studied a single frequency refractive index sensor based on a finite one-dimensional photonic crystals with two non-identical defects.

Physics Department, Faculty of Sciences, Benha University, Benha, Egypt
Email: said.alsayed@fsc.bu.edu.eg
Received: xx Xxxx xxxx
Accepted: xx Xxxx xxxx

The aim of the present work is to investigate and analyze the photonic band gap in T-tuning filter. I'm considered the defected photonic crystals of the form air $(Si/SiO_2)^N$ D_1 $(Si/SiO_2)^M$ D_2 $(Si/SiO_2)^L$ Glass, as one dimensional photonic crystal. I'm studied the transmission of the electromagnetic wave in Uv, visible and infrared (IR) regions under the effect of variation temperature for different types of the second defect D_2.

Where the incident light on the first nano-layer of Si, leads to an emitted spectra from silicon which incident on the second layer and so on up to finally transmitted from the substrate. The relation between the transmitted spectra and the wavelength is figured.

The calculations show that the position of PBG can be changed by changing the temperature. Also the PBG will be shifted by variation of the thickness and the type of the second defected layer. The analysis of the present work was calculated by using the transfer matrix method TMM through the Mat lab software.[19]

2. THEORETICAL BACKGROUND

Figure 1 shows 1D-periodic structure in the form air $(AB)^N$ D_1 $(AB)^M$ D_2 $(AB)^L$ d_s, in which the thicknesses of the four constituent layers are denoted by d_1, d_2, d_{d1}, d_{d2} and d_s. The corresponding refractive indices are separately indicated by n_0, n_1, n_2, n_{d1}, n_{d2} and n_s, where $n_0 = 1$ is taken for free space and n_s is for the substrate and double defect layers in the middle of the three periodic.

The first defect $Bi_4Ge_3O_{12}$ is sandwitached between the first tow periods of Si and SiO_2. Here, we set $n_{d1} = 2.05$, and $d_{d1} = d_1$. In addition, the thermo-optic coefficient and the thermal expansion coefficient for $Bi_4Ge_3O_{12}$ are $3.5 \times 10^{-5}/°C$ and $6.3 \times 10^{-6}/°C$ respectively, where the different dielectric media, Si ($n_1 = 3.3$), SiO_2 ($n_2 = 1.46$) and $M = N = L = 10$ layer.[20] Here, we set the thermo-optic coefficients for Si and SiO_2 are $1.86 \times 10^{-4}/°C$ and $6.8 \times 10^{-6}/°C$, respectively.[21] The thermal expansion coefficients for Si and SiO_2 are $0.5 \times 10^{-6}/°C$ and $2.6 \times 10^{-6}/°C$, respectively. The substrate is taken to be glass with a refractive index of $n_s = 1.5$. The type and the thickness of the second defect are become variable.

In the present calculations, focusing on the variation of both the number and the positions of the PBG characteristics induced by changing the optical path of the structure under the effect of temperature.

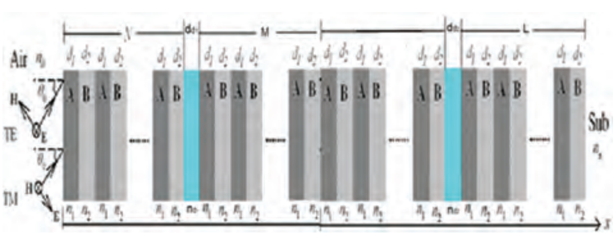

Fig. 1.

The thickness and the refractive index can be changed due to the thermal expansion and the thermo-optic effect as follows:[22]

$$d = d_o + \alpha d_o \Delta T \tag{1}$$

where (d_o) is the thickness of the layer at room temperature, α is the thermal expansion coefficient of the medium and ΔT is the variation of the temperature. The refractive index of the medium is dependent on temperature according the thermo-optical effect as follows,

$$n = n_o + \beta n_o \Delta T \tag{2}$$

Where n_o is the refractive index at room temperature and β is the thermo-optic coefficient.

Let us generalized the electromagnetic waves propagation through the multilayer structure along x-direction can be written as:

$$n(x) = \begin{cases} n_0 & x < x_o \\ n_1 & x_o < x < x_1 \\ n_2 & x_1 < x < x_2 \\ \vdots & \vdots \\ n_s & x_{2N} < x \end{cases} \tag{3}$$

The electric field vector of a general plane-wave solution of the wave equation to periodic structure can be written as:

$$E = E(x) e^{i(\omega t - \beta z)} \tag{4}$$

Where β is the z-component of the wave vector which given by:

$$\beta = n_m \frac{\omega}{c} \sin\theta_m, \quad m = 0, 1, 2, 3, \ldots \tag{5}$$

θ_m is the angle of the incident wave in each layer and c is the speed of light. The electric field distribution $E(x)$ can be written as:

$$E(x) = \begin{cases} A_o e^{-ik_{ox}(x-x_o)} + B_o e^{ik_{ox}(x-x_o)} & x < x_o \\ A_1 e^{-ik_{1x}(x-x_1)} + B_1 e^{ik_{1x}(x-x_1)} & x_o < x < x_1 \\ A_2 e^{-ik_{2x}(x-x_2)} + B_2 e^{ik_{2x}(x-x_2)} & x_1 < x < x_2 \\ A'_2 e^{-ik_{2x}(x-x_2)} + B'_2 e^{ik_{2x}(x-x_2)} & x > x_2 \end{cases} \tag{6}$$

where A_m and B_m are the amplitude of the plane wave at each interface $x = x_m$, k_{mx} is the wave vector of the x-component, $k_{mx} = n_m(\omega/c)\cos\theta_m$ the amplitudes of the plane waves at different layers for N period are related by:[20]

$$\begin{pmatrix} A_m \\ B_m \end{pmatrix} = D_m^{-1} D_{m+1} \begin{pmatrix} A'_{m+1} \\ B'_{m+1} \end{pmatrix} = D_m^{-1} D_{m+1} P_{m+1} \begin{pmatrix} A_{m+1} \\ B_{m+1} \end{pmatrix} \tag{7}$$

with $m = 0, 1, 2, \ldots, 2N$. The dynamical matrices D for the TE wave and TM wave can be written as:

$$D_m = \begin{pmatrix} 1 & 1 \\ n_m \cos\theta_m & -n_m \cos\theta_m \end{pmatrix} \quad \text{for TE waves } (S \text{ wave}) \tag{8a}$$

and

$$D_m = \begin{pmatrix} \cos\theta_m & \cos\theta_m \\ n_m & -n_m \end{pmatrix} \quad \text{for TM waves } (P \text{ wave}) \tag{8b}$$

For simplifying, the propagation matrix P_m can be written as a function of sine and cosine instead of the exponential function as:

$$P_m = \begin{pmatrix} \cos\varphi_l + i\sin\varphi_l & 0 \\ 0 & \cos\varphi_l - i\sin\varphi_l \end{pmatrix} \tag{9}$$

where the phase change of the wave propagating through any layer is φ_l which can be given by:

$$\varphi_l = \frac{2\pi n_l d_l}{\lambda}\cos\theta_l, \quad (l = 1, 2, 3, \ldots)$$

Where n_l and d_l are the refractive index and thickness of the layers respectively.

The relation between the forward traveling amplitudes and the backward traveling amplitudes of the plane wave can be given by:

$$\begin{pmatrix} A_o \\ B_o \end{pmatrix} = M(a)\begin{pmatrix} A'_2 \\ B'_2 \end{pmatrix} = D_1 P_1 D_1{}^{-1} D_2 P_2 D_2^{-1} \tag{10}$$

with

$$M(a) = \begin{pmatrix} m_{11} & m_{12} \\ m_{21} & m_{22} \end{pmatrix} \tag{11}$$

Where (a), is the transfer matrix for a single period system, m_{11}, m_{12}, m_{21} and m_{22} are computed for TE-waves and TM-waves using the same analysis stated above, where the lattice constant is $a = (d_1 + d_2)$. By using the inversion matrix and redistribution Eq. (10) for N waves, the matrix elements can be obtained as:

$$\begin{aligned} m_{11} &= (\cos\varphi_1 \cos\varphi_2) - \frac{n_2\cos\theta_2}{n_1\cos\theta_1}(\sin\varphi_1 \sin\varphi_2), \\ m_{12} &= \frac{i}{n_2\cos\theta_2}(\cos\varphi_1 \sin\varphi_2 + \frac{i}{n_1\cos\theta_1}(\sin\varphi_1\cos\varphi_2), \\ m_{21} &= in_1\cos\theta_1(\sin\varphi_1\cos\varphi_2) + in_2\cos\theta_2(\sin\varphi_2\cos\varphi_1), \\ m_{22} &= (\cos\varphi_1\cos\varphi_2) - \frac{n_1\cos\theta_1}{n_2\cos\theta_2}(\sin\varphi_1\sin\varphi_2) \end{aligned} \tag{12}$$

The transfer matrix for N periodic structure can be taken the form:[23]

$$M_T(Na) = M(Na) = (M(a))^N = \begin{pmatrix} M_{11} & M_{12} \\ M_{21} & M_{22} \end{pmatrix} = \begin{pmatrix} m_{11} & m_{12} \\ m_{21} & m_{22} \end{pmatrix}^N \tag{13a}$$

Since,

$$M(Na) = D_o^{-1}\begin{pmatrix} Q_{11} & Q_{12} \\ Q_{21} & Q_{22} \end{pmatrix} D_s = D_o^{-1}\left(\prod_{k=1}^{N} D_K P_K D_K{}^{-1} D_{K+1} P_{K+1} D_{k+1}^{-1}\right) D_s \tag{13b}$$

The relation between the elements of the matrix for N periods, Q_{11}, Q_{12}, Q_{21} and Q_{22} and the elements of the single period matrix (m_{11}, m_{12}, m_{21} and m_{22}) can take the following form.[24]

$$Q_{11} = m_{11}U_{N-1}(\psi) - U_{N-2}(\psi), \quad Q_{12} = m_{12}U_{N-1}(\psi)$$
$$Q_{21} = m_{21}U_{N-1}(\psi) \quad \text{and} \quad Q_{22} = m_{22}U_{N-1}(\psi) - U_{N-2}(\psi) \tag{14}$$

Where $U_N(\psi)$, is the second kind of Chebyshev polynomials which is given as:

$$U_N(\psi) = \frac{\sin((N+1)\cos^{-1}\psi)}{\sqrt{1-\psi^2}}, \quad \text{and} \quad \psi = 0.5(m_{11} + m_{22}) \tag{15}$$

For our structure air $(\text{AB})^N D_1$ $(\text{AB})^M D_2$ $(\text{AB})^L$ glass, the general form can be written as:

$$M_{\text{structure}} = \begin{pmatrix} M_{11} & M_{12} \\ M_{21} & M_{22} \end{pmatrix} = D_o^{-1}\begin{bmatrix} \left(\prod_{k=1}^{N} D_K P_K D_K^{-1} D_{K+1} P_{K+1} D_{k+1}^{-1}\right)\begin{pmatrix} d_{11} & d_{12} \\ d_{21} & d_{22} \end{pmatrix} \\ \left(\prod_{k=1}^{M} D_K P_K D_K^{-1} D_{K+1} P_{K+1} D_{k+1}^{-1}\right)\begin{pmatrix} d'_{11} & d'_{12} \\ d'_{21} & d'_{22} \end{pmatrix} \\ \left(\prod_{k=1}^{L} D_K P_K D_K^{-1} D_{K+1} P_{K+1} D_{k+1}^{-1}\right) \end{bmatrix} D_s \tag{16}$$

The third and the fifth matrices can be obtained by using the same above equations, except for the changing of the period number from N to M and L. The second and fourth matrices are for the first and second defected layers. Then the components of the defect layer matrix can be calculated separately to take the form,

$$D = (D_d P_d D_d^{-1}) = \begin{pmatrix} \cos\varphi_d & i\sin\varphi_d / n_d\cos\theta_d \\ in_d\cos\theta_d\sin\varphi_d & \cos\varphi_d \end{pmatrix} \tag{17}$$

Where: φ_d is the angle phase difference of light propagates through any defected layer $\varphi_d = (2\pi n_d d_d/\lambda)\cos\theta_d$, θ_d is the incident angle in the defected layers, n_d and d_d are the refractive index and thickness of the defected layers respectively.

Then using these matrices, one can calculate M_{11}, M_{12}, M_{21} and M_{22} components.

The reflection coefficient r and the transmission coefficient t, can be obtained as:

$$r = \frac{M_{21}}{M_{11}}, \quad \text{and} \quad t = \frac{1}{M_{11}}$$

Finally the reflectance and the transmittance are given by

$$R = |r^2|, \quad T = \frac{f_s}{f_0}|t^2| \tag{18}$$

Where, the expressions for f_0 and f_s are defined as following:

$$f_0 = \sqrt{\frac{\varepsilon_0}{\mu_0}} n_0 \cos\theta_0 \quad \text{and} \quad f_s = \sqrt{\frac{\varepsilon_0}{\mu_0}} n_s \cos\theta_s$$

3. RESULTS AND DISCUSSION

The numerical results of TE wave's propagation through the 1D PCs under Uv, visible up to far IR radiation are presented. The analysis was investigated by studying the transmittance characteristics of 1D as a function of the wavelength under the effect of temperature above ambiant.

Figure 2 illustrates the transmittance spectrum as a function of wavelength taking into account all the previous conditions in Figure 1 considering the second defect is Si ($d_1 = d_{d1} = d_{d2} = 117$ nm, $d_2 = 265$ nm) at different temperatures 125 °C, 325 °C, 525 °C and 725 °C, respectively. The figure shows that, the number of photonic band gaps and their widths were increased by increasing the temperature above room temperature. At 125 °C there are three PBG in Uv range, two PBG in IR and it shows one wide PBG in the range of far IR. For further increases in the temperature, the number of PBG increases, becomes wider and expands towards the far IR due to the effect of thermo-optic effect. This was attributed to the fact that, to obtain stable interference, the phase difference should be constant, so the ratio between the optical path and the wavelength should be constant, so the PBG should be shifted to higher values of wavelengths

Figures 3–5 illustrate the relation between the transmission spectrum with the incident wavelength for the same conditions of Figure 2, considering the thickness of the second defect equals to ($d_1/4$ nm, $d_1/6$ nm and $d_1/8$ nm), respectively. These figures show the same behavior as that in Figure 2 but hear, there were sharp peaks at the end of

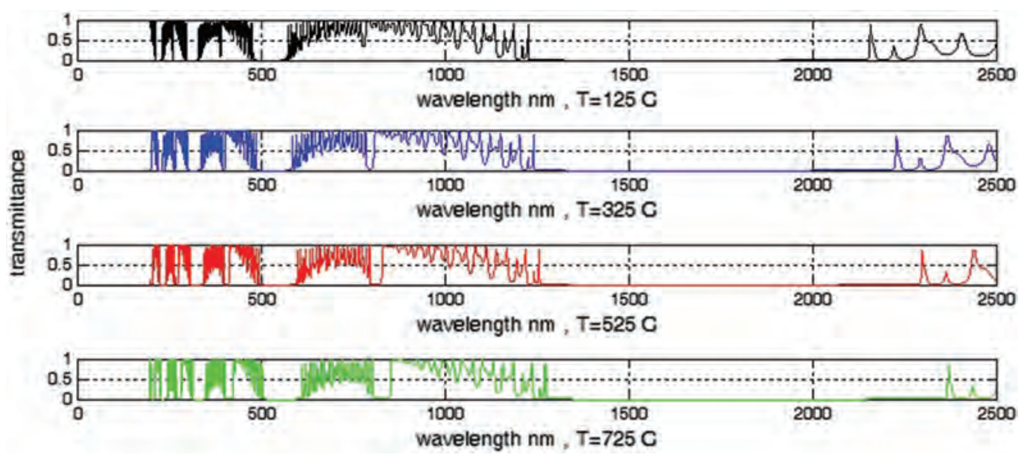

Fig. 2. Transmission spectra for the defected 1D PCs at normal incidence, in Uv, visible and IR spectra of air $(Si/SiO_2)^N$ D_1 $(Si/SiO_2)^M$ D_2 $(Si/SiO_2)^L$ glass structure for $d_1 = 117$ nm, $d_2 = 265$ nm, D_1 is $Bi_4Ge_3O_{12}$, D_2 is Si, $d_{d1} = d_1$ and $d_{d2} = d_1$ at different values of temperatures.

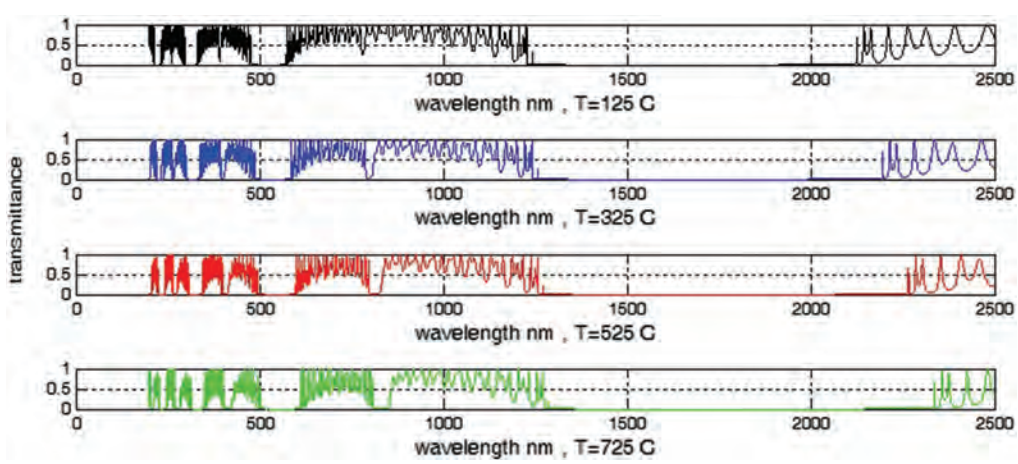

Fig. 3. Transmission spectra for the defected 1D PCs at normal incidence, in Uv, visible and IR spectra of air $(Si/SiO_2)^N D_1$ $(Si/SiO_2)^M D_2$ $(Si/SiO_2)^L$ glass structure for $d_1 = 117$ nm, $d_2 = 265$ nm, $d_{d1} = d_1$, D_1 is $Bi_4Ge_3O_{12}$, D_2 is Si and $d_{d2} = d_1/4$ at different values of temperatures.

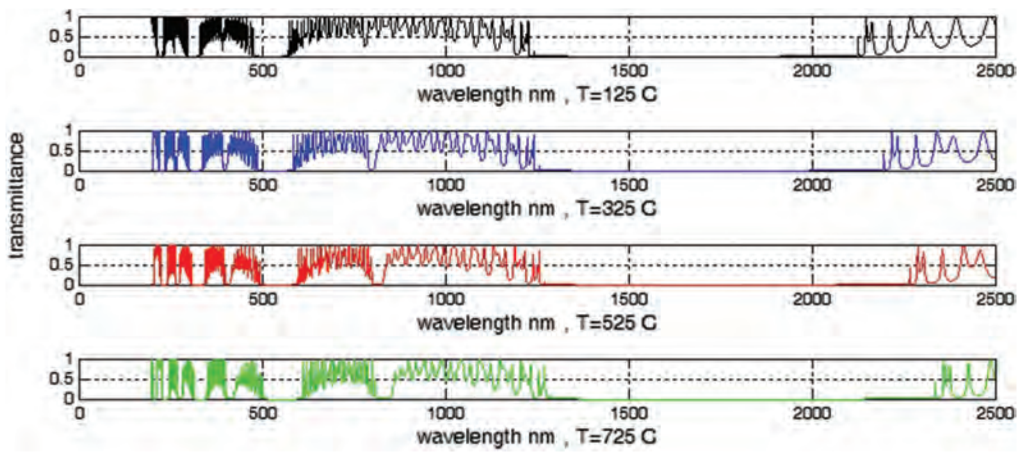

Fig. 4. Transmission spectra for the defected 1D PCs at normal incidence, in Uv, visible and IR spectra of air $(Si/SiO_2)^N D_1$ $(Si/SiO_2)^M D_2$ $(Si/SiO_2)^L$ glass structure for $d_1 = 117$ nm, $d_2 = 265$ nm, $d_{d1} = d_1$, D_1 is $Bi_4Ge_3O_{12}$, D_2 is Si and $d_{d2} = d_1/6$ at different values of temperatures.

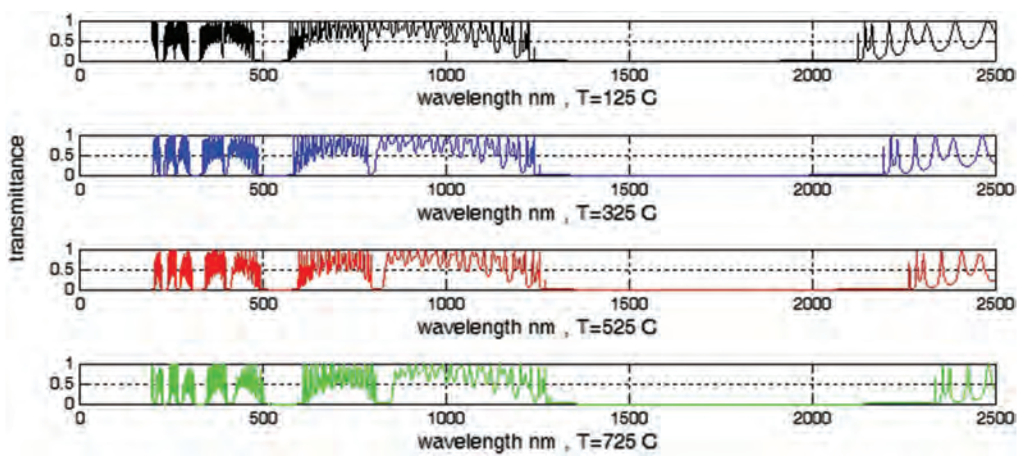

Fig. 5. Transmission spectra for the defected 1D PCs at normal incidence, in Uv, visible and IR spectra of air $(Si/SiO_2)^N D_1$ $(Si/SiO_2)^M D_2$ $(Si/SiO_2)^L$ glass structure for $d_1 = 117$ nm, $d_2 = 265$ nm, $d_{d1} = d_1$, D_1 is $Bi_4Ge_3O_{12}$, D_2 is Si and $d_{d2} = d_1/8$ at different values of temperatures.

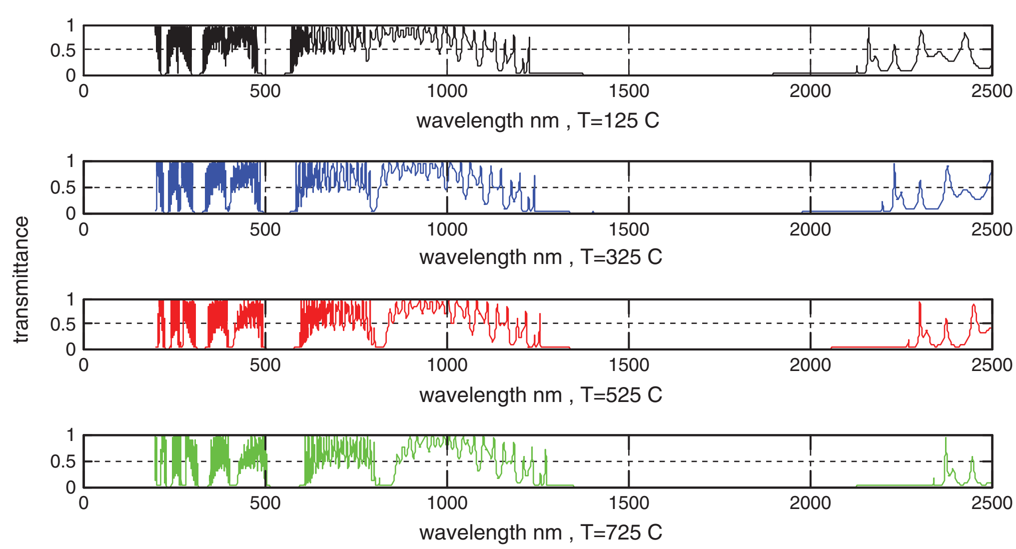

Fig. 6. Transmission spectra for the defected 1D PCs at normal incidence, in Uv, visible and IR spectra of air $(Si/SiO_2)^N$ D_1 $(Si/SiO_2)^M$ D_2 $(Si/SiO_2)^L$ glass structure for $d_1 = 117$ nm, $d_2 = 265$ nm, $d_{d1} = d_1$, D_1 is $Bi_4Ge_3O_{12}$, D_2 is Si and $d_{d2} = d_2$ at different values of temperatures.

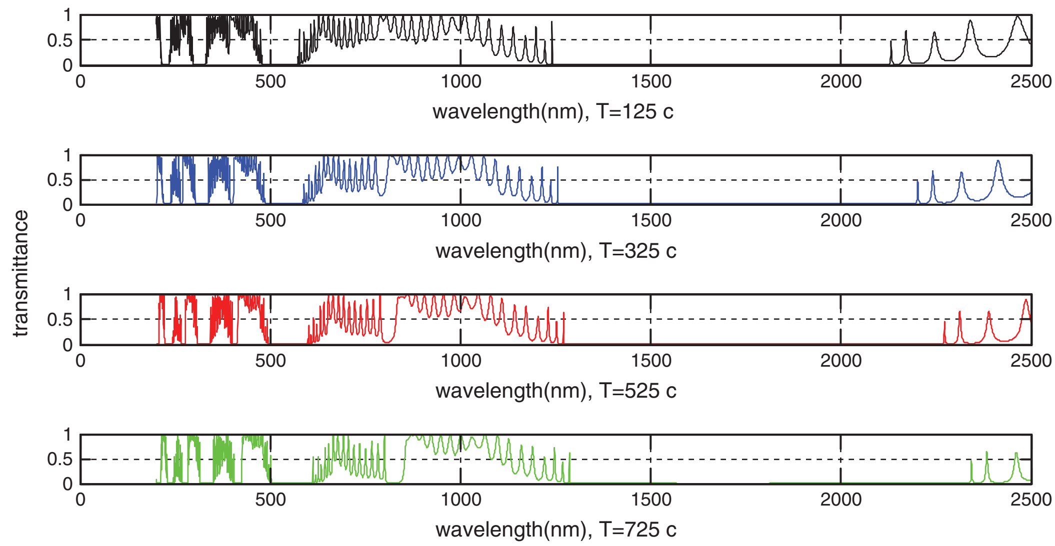

Fig. 7. Transmission spectra for the defected 1D PCs at normal incidence, in Uv, visible and IR spectra of air $(Si/SiO_2)^N$ D_1 $(Si/SiO_2)^M$ D_2 $(Si/SiO_2)^L$ glass structure for $d_1 = 117$ nm, $d_2 = 265$ nm, $d_{d1} = d_1$, D_1 is $Bi_4Ge_3O_{12}$, D_2 is SiO_2 and $d_{d2} = d_1$ at different values of temperatures.

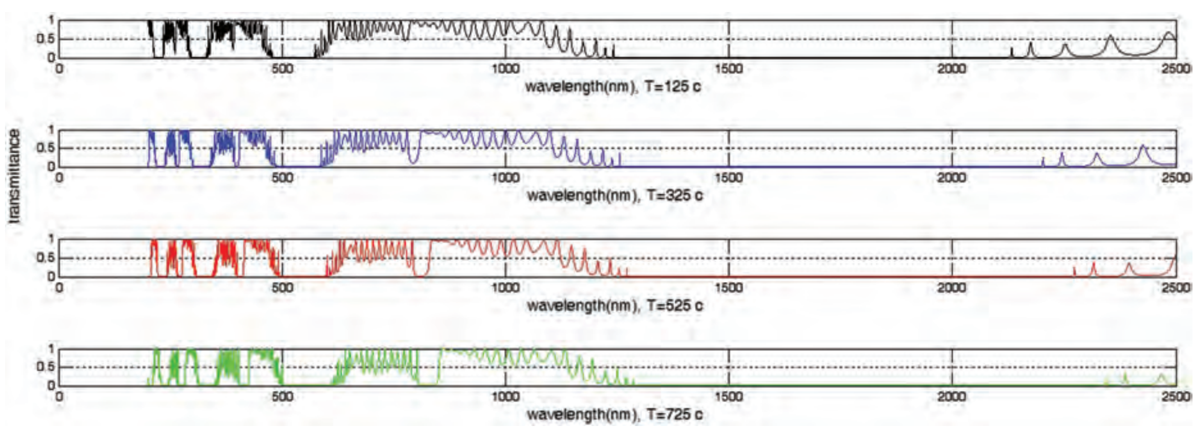

Fig. 8. Transmission spectra for the defected 1D PCs at normal incidence, in Uv, visible and IR spectra of air $(Si/SiO_2)^N$ D_1 $(Si/SiO_2)^M D_2$ $(Si/SiO_2)^L$ glass structure for $d_1 = 117$ nm, $d_2 = 265$ nm, $d_{d1} = d_1$, D_1 is $Bi_4Ge_3O_{12}$, D_2 is SiO_2 and $d_{d2} = d_2$ at different values of temperatures.

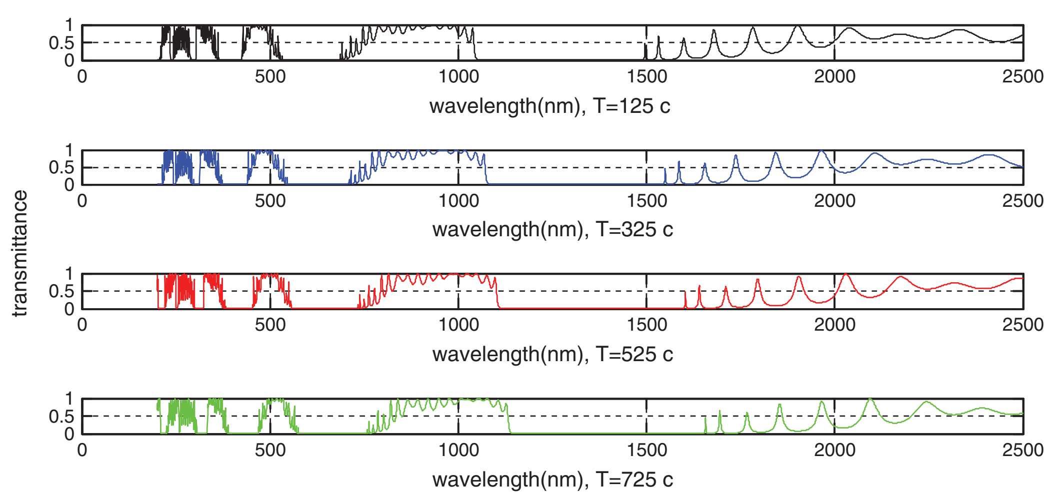

Fig. 9. Transmission spectra for the defected 1D PCs at normal incidence, in Uv, visible and IR spectra of air $(Si/SiO_2)^N D_1$ $(Si/SiO_2)^M$ D_2 $(Si/SiO_2)^L$ glass structure for $d_1 = 137$ nm, $d_2 = 90$ nm, $d_{d1} = d_1$, D_1 is $Bi_4Ge_3O_{12}$, D_2 is SiO_2 and $d_{d2} = d_2$ at different values of temperatures.

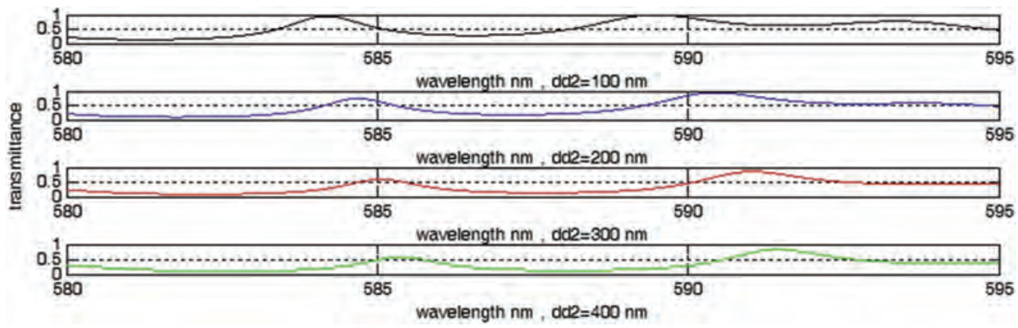

Fig. 10. Transmission spectra for the defected 1D PCs at normal incidence, in Uv, visible and IR spectra of air $(Si/SiO_2)^N$ D_1 $(Si/SiO_2)^M$ D_2 $(Si/SiO_2)^L$ glass structure for $d_1 = 117$ nm, $d_2 = 265$ nm, $d_{d1} = d_1$, D_1 is $Bi_4Ge_3O_{12}$, D_2 is Si, $T = 25$ °C and different values of the second defect d_{d2}.

the final PBG with transmittance equals to 40%, 55% and 80% at the same temperature, respectively. Also Figure 4 shows a sharp transmission peak at 125 °C with 20% at the beginning of the final PBG and this value is increasing up to 50% when the thickness of the second defect equals to $d_1/8$. These harp peaks are very important for laser applications.

By increasing the width of second defect to 265 nm, at the same conditions of Figure 2, the behavior of the transmittance as a function of wavelength is the same as that in Figure 2 but the calculations illustrate the sharp peak at the end of the final PBG with 20% of the maximum transmittance. These results are illustrated in Figure 6.

If the second defect is changed from Si to SiO_2 for the same conditions of Figure 2, the transmittance as a function of wavelength is illustrated in Figure 7, for different temperatures 125 °C, 325 °C, 525 °C and 725 °C, respectively. The figure shows that, the number of PBG was increased with increasing the temperature from 4 PBG at 125 °C to 6 at 325 °C and 7 PBG at 725 °C. Also the spectrum was shifted to higher values of wavelength by increasing the temperature values. The figure illustrate also that the sharp peaks at the beginning of the final PBG with transmittance approximately in the range of 60–80%.

Figure 8 illustrate, for the same conditions of Figure 7 at $d_{d2} = d_2 = 265$ nm, the transmittance of the photonic crystal in one direction, as a function of the wavelength. The figure shows the same behavior as that in Figure 7 but the sharp peaks were in the range of transmittance from 40% at 125 °C to 20% at 725 °C.

Figure 9 shows the transmittance as a function of wavelength for different temperatures 125 °C, 325 °C, 525 °C and 725 °C, respectively, at the same conditions of Figure 8 considering $d_1 = 137$ nm and $d_2 = d_{d2} = 90$ nm. The figure shows the same behavior as that in Figure 8, but the shift in PBG was larger than that in Figure 8. Also the number of PBG in between 1500 nm to 2500 nm was larger than that in Figure 8. Also the figure shows no sharp peaks in the final PBG as in Figures 7 and 8.

Figure 10 shows the relation between the transmission spectrum with the incident wavelength for the same conditions of Figure 2, considering the thickness of the second defect equal to (100 nm, 200 nm, 300 nm and 400 nm) respectively at 25 °C above ambiant. The figure shows that the peak of the transmittance was equal to nearly 1 at $d_{d2} = 100$ nm and decreased and shifted to larger values of wavelength by increasing the thickness of the second defect.

Figure 11 shows the relation between the transmission spectrum, for the same conditions of Figure 2, with d_{d2} considering wavelength $\lambda = 580$ nm at different values of temperatures (50 °C, 100 °C, 150 °C and 200 °C) above ambiant respectively. The figure shows that, the number of peaks were the same but the sharpness of the peaks and the completely PBG was obtained by increasing the temperature up to 150 °C. Where the transmittance is given

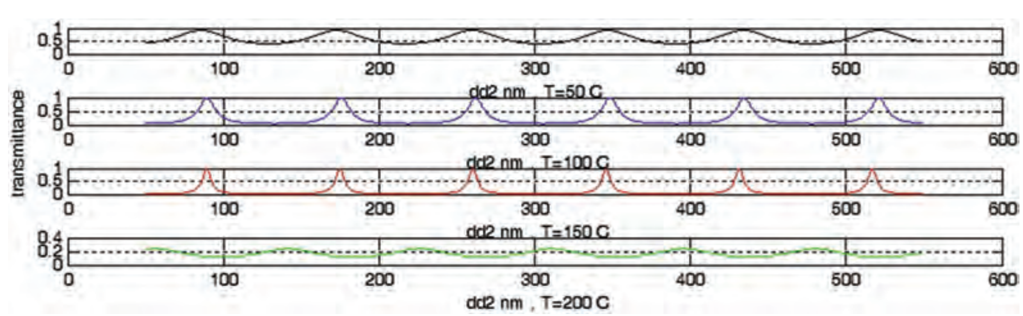

Fig. 11. Transmission spectra for the defected 1D PCs at normal incidence, in Uv, visible and IR spectra of air $(Si/SiO_2)^N$ D_1 $(Si/SiO_2)^M$ D_2 $(Si/SiO_2)^L$ glass structure for $d_1 = 117$ nm, $d_2 = 265$ nm, $d_{d1} = d_1$, D_1 is $Bi_4Ge_3O_{12}$, D_2 is Si, wavelength = 580 nm, at different values of the second defect d_{d2} and different temperatures.

by 100% at 150 °C and decreases by more increasing the temperature.

From Figures 2–11 variable filters in Uv, visible and IR can be done, because the position of the photonic band gap can be shifted by changing the temperature and the type of the second defect. The second defect D_2 can be taken different types such as Si or SiO_2 or another, this leads to different filters and sensors.

4. CONCLUSIONS

A theoretical analysis of the transmission properties in Uv, visible and IR regions for 1D PCs has been investigated in the presence of temperature variations. The main final results were:

1—The numerical calculations for 1D PC show that, the PBG increased by increasing the temperature and the PBG shifted to large values of wavelength, this was due to the change in the contrast between the refractive indices of the constituent materials.

2—By changing the thickness of the second defect at constant value of the wavelength, the width of transmitted spectrum decreased and the number of pure PBG increased by increasing the temperature.

3—Different ranges of PBG in which the photons with certain frequencies can't propagate inside the photonic crystal, gives more stop bands which may be useful in many applications such as filters and electromagnetic waves sensors.

References and Notes

1. Y. Fink, J. N. Winn, S. Fan, C. Chen, J. Michel, J. D. Joannopoulos, and E. L. Thomas, *Science* 282, 1679 **(1998)**.
2. K. Miura, J. Qiu, S. Fujiwara, S. Sakaguchi, and K. Hirao, *Appl. Phys. Lett.* 80, 2263 **(2002)**.
3. J. Qiu, X. Jiang, C. Zhu, H. Inouye, J. Si, and K. Hirao, *Opt. Lett.* 29, 370 **(2004)**.
4. C. Kittel, Introduction to Solid State Physics, John Wiley & Sons, Inc., New York **(1976)**.
5. B. Suthar, V. Kumar, A. Kumar, K. S. Singh, and A. Bhargava, *Progress in Electromagnetics Research Letters* 27, 43 **(2011)**.
6. A. Bhargava and B. Suthar, *Journal of Ovonic Research* 5, 187 **(2009)**.
7. B. Li, J. Zhou, L. Li, X. J. Wang, X. H. Liu, and J. Zi, *Appl. Phys. Lett.* 83, 4704 **(2003)**.
8. V. Kumar, K. S. Singh, S. K. Singh, and S. P. Ojha, *Progress in Electromagnetic Research M* 14, 101 **(2010)**.
9. Arafa H. Aly and Sang-Wanryu, *International Journal of Modern Physics B* 23, 2297 **(2009)**.
10. Arafa. H. Aly, S. E.-S. Abdel Ghany, and B. M. Kamal, *International Journal of Advances in Engineering and Technology* 8, 59 **(2015)**.
11. P. Lodahl, A. F. Van Driel, I. S. Nikolaev, A. Irman, K. Overgaag, D. L. Vanmaekelbergh, and W. L. Vos, *Nature* 430, 654 **(2004)**.
12. M. J. Ventura and M. Gu, *Adv. Mater.* 20, 1329 **(2008)**.
13. G. Kristina, Technology Review, The Authority of the future of technology.web.13feb.2011.http://technologyreview/computing/20840.
14. P. Yeh, Optical Waves in Layered Media, Wiley, New York **(1988)**.
15. V. C. Gungor and G. P. Hancke, *IEEE Transaction on industrial Electronics* 56, 4258 **(2009)**.
16. K. Kaviyarasu, A. Ayeshamariam, E. Manikandan, J. Kennedy, R. Ladchumananandasivam, U. U. Gomes, M. Jayachandran, and M. Maaza, *Materials Science and Engineering B* 10, 1 **(2016)**.
17. J. Kennedy, G. V. M. Williams, P. P. Murmu, and B. J. Ruck, *Phys. Rev. B* 88, 214423 **(2013)**.
18. H. Alatas, H. Mayditia, H. Hardhienata, A. A. Iskandar, and M. O. Tjia, *Japanese Journal of Applied Physics* 45, 6754 **(2006)**.
19. S. Dang, *Opt. Rev.* 15, 255 **(2008)**.
20. Arafa. H. Aly, S. E.-S. Abd El Ghany, M. M. Fadlallah, E. Salman, and B. M. Kamal, *Journal of Nanoelectronics and Optoelectronics* 10, 1 **(2015)**.
21. Arafa H. Aly and M. Doaa, *Journal of Multidisciplinary Engineering Science and Technology* 1, 77 **(2014)**.
22. M. Tinkham, Introduction to Superconductivity, Znded. McGraw-Hill, New York **(1996)**.
23. S. John, *Phys. Rev. Lett.* 58, 2486 **(1987)**.
24. J. P. Mckelvey (ed.), Solid State and Semiconductor Physics, Harper and Row **(1966)**.